Magnetic Fields in Galaxies

Rainer Beck

Space Science Reviews

ISSN 0038-6308
Volume 166
Combined 1-4

Space Sci Rev (2012) 166:215-230
DOI 10.1007/s11214-011-9782-z

Springer

Space Sci Rev (2012) 166:215–230
DOI 10.1007/s11214-011-9782-z

Magnetic Fields in Galaxies

Rainer Beck

Received: 13 December 2010 / Accepted: 15 April 2011 / Published online: 19 May 2011

Abstract Radio synchrotron emission, its polarization and its Faraday rotation are powerful tools to study the strength and structure of magnetic fields in galaxies. Unpolarized emission traces turbulent fields which are strongest in spiral arms and bars (20–30 μG) and in central starburst regions (50–100 μG). Such fields are dynamically important, e.g. they can drive gas inflows in central regions. Polarized emission traces ordered fields which can be regular or anisotropic random, generated from isotropic random fields by compression or shear. The strongest ordered fields of 10–15 μG strength are generally found in interarm regions and follow the orientation of adjacent gas spiral arms. Ordered fields with spiral patterns exist in grand-design, barred and flocculent galaxies, and in central regions of starburst galaxies. Faraday rotation measures (RM) of the diffuse polarized radio emission from the disks of several spiral galaxies reveal large-scale patterns, which are signatures of regular fields generated by a mean-field dynamo. However, in most spiral galaxies observed so far the field structure is more complicated. Ordered fields in interacting galaxies have asymmetric distributions and are an excellent tracer of past interactions between galaxies or with the intergalactic medium. Ordered magnetic fields are also observed in radio halos around edge-on galaxies, out to large distances from the plane, with X-shaped patterns. Future observations of polarized emission at high frequencies, with the EVLA, the SKA and its precursors, will trace galactic magnetic fields in unprecedented detail. Low-frequency telescopes (e.g. LOFAR and MWA) are ideal to search for diffuse emission and small RMs from weak interstellar and intergalactic fields.

Keywords Synchrotron emission · Radio telescopes · Faraday rotation · Dynamo action · Galaxies: spiral structure · Galaxies: magnetic fields

1 Introduction

Magnetic fields are a major agent in the interstellar medium and also control the density and distribution of cosmic rays. Cosmic rays accelerated in supernova remnants can provide

R. Beck (✉)
Max-Planck-Institut für Radioastronomie, Auf dem Hügel 69, 53121 Bonn, Germany
e-mail: rbeck@mpifr-bonn.mpg.de

the pressure to drive galactic outflows and buoyant loops of magnetic fields via the Parker instability. Outflows from starburst galaxies in the early Universe may have magnetized the intergalactic medium.

The detection of ultrahigh-energy cosmic rays (UHECRs) with the AUGER observatory and the anisotropic distribution of their arrival directions (Abreu et al. 2010) calls for a proper model of particle propagation. As UHECR particles are deflected by large-scale regular fields and scattered by turbulent fields, the structure and the extent of the fields in the disk and halo of the Milky Way need to be known, but the present data do not allow safe conclusions (Noutsos, this issue). The view onto external spiral galaxies can help to model the field structure of the Milky Way.

2 Origin of Magnetic Fields

In spite of our increasing knowledge of cosmic magnetic fields, many important questions, especially their origin and evolution, their strength and structure in intergalactic space, their first occurrence in young galaxies, and their dynamical importance for galaxy evolution remain unanswered.

The origin of the first magnetic fields in the Universe is a mystery (Widrow 2002). *Seed fields* may be "primordial", generated during a phase transition in the early Universe (Caprini et al. 2009), or originate from the time of cosmological structure formation by the Weibel instability (Lazar et al. 2009), or from injection by the first stars or jets generated by the first black holes (Rees 2005), or from the Biermann mechanism in the first supernova remnants (Hanayama et al. 2005). The strength of intergalactic fields is at least 10^{-16} G and their filling factor is larger than 60%, as derived from high-energy γ-ray observations with HESS and FERMI which indicate that the secondary particles are deflected by the intergalactic fields (Dolag et al. 2011).

The most promising mechanism to sustain magnetic fields in the interstellar medium of galaxies is the dynamo (Beck et al. 1996) (see also Brandenburg et al., this issue). A small-scale dynamo in protogalaxies may have amplified seed fields to several μG strength (the energy level of turbulence) within less than 10^8 yr (Schleicher et al. 2010). To explain the generation of large-scale fields in galaxies, the mean-field dynamo has been developed. It is based on turbulence, differential rotation and helical gas flows (α-*effect*), driven by supernova explosions (Gressel et al. 2008). The mean-field dynamo in galaxy disks predicts that within a few 10^9 yr large-scale regular fields are generated from μG turbulent fields (Arshakian et al. 2009), forming spiral patterns (*modes*) with different azimuthal symmetries in the disk and vertical symmetries in the halo (see Sect. 6.1). Global numerical models of galaxies (Gissinger et al. 2009; Hanasz et al. 2009) confirm the basic results of the mean-field approximation.

The mean-field dynamo generates large-scale helicity with a non-zero mean in each hemisphere. As total helicity is a conserved quantity, the dynamo is quenched by the small-scale fields with opposite helicity unless these are removed from the system (Shukurov et al. 2006). Outflows are probably essential for effective mean-field dynamo action.

3 Measuring Magnetic Fields in Galaxies

Magnetic fields need illumination to be detectable. *Polarized emission* at optical, infrared, submillimeter and radio wavelengths holds the clue to measure magnetic fields in galaxies.

Optical linear polarization is a result of extinction by elongated dust grains in the line of sight which are aligned in the interstellar magnetic field (the *Davis-Greenstein effect*). The E-vector runs parallel to the field. However, light can also be polarized by scattering, a process unrelated to magnetic fields and hence a contamination that is difficult to subtract from the diffuse polarized emission from galaxies, e.g. in M 51 (Scarrott et al. 1987). Optical polarization data of about 5500 selected stars in the Milky Way yielded the orientation of the large-scale magnetic field near the sun (Fosalba et al. 2002). Together with measurements of stellar distances, a 3-D analysis of the magnetic field within about 5 kpc from the sun is possible, but more data are needed.

Linearly polarized emission from elongated dust grains at infrared and submillimeter wavelengths is not affected by polarized scattered light. The B-vector is parallel to the magnetic field. The field structure can be mapped in gas clouds of the Milky Way (Tang et al. 2009) and in galaxies, e.g. in the halo of M 82 (Greaves et al. 2000).

Most of what we know about interstellar magnetic fields comes through the detection of radio waves. *Zeeman splitting* of radio spectral lines directly measures the field strength in gas clouds of the Milky Way (Heiles, this issue) and in starburst galaxies (Robishaw et al. 2008). The intensity of *synchrotron emission* is a measure of the number density of cosmic-ray electrons in the relevant energy range and of the strength of the total magnetic field component in the sky plane. The assumption of energy equipartition between these two components allows us to calculate the total magnetic field strength from the synchrotron intensity (see Sect. 4.1).

Linearly polarized synchrotron emission emerges from ordered fields in the sky plane. As polarization "vectors" are ambiguous by 180°, they cannot distinguish *regular (coherent) fields*, defined to have a constant direction within the telescope beam, from *anisotropic fields*, which are generated from turbulent fields by compressing or shearing gas flows and frequently reverse their direction within the telescope beam. Unpolarized synchrotron emission indicates *turbulent (random) fields* which have random directions in 3-D and have been amplified and tangled by turbulent gas flows.

The intrinsic degree of linear polarization of synchrotron emission is about 75%. The observed degree of polarization is smaller due to the contribution of unpolarized thermal emission, which may dominate in star-forming regions, by *Faraday depolarization* along the line of sight and across the beam (Sokoloff et al. 1998), and by geometrical depolarization due to variations of the field orientation within the beam.

The polarization vector is rotated in a magnetized thermal plasma by *Faraday rotation*. If Faraday rotation is small (in galaxies typically at wavelengths shorter than a few centimeters), the B-vector of polarized emission gives the intrinsic field orientation in the sky plane, so that the magnetic pattern can be mapped directly (Beck 2005). The rotation angle is proportional to the square of the wavelength λ^2 and to the *Rotation Measure (RM)*, which is related to the *Faraday depth (FD)*, see below. As the rotation angle is sensitive to the sign of the field direction, only regular fields give rise to Faraday rotation, while anisotropic and random fields do not. Measurements of the Faraday rotation from multi-wavelength observations allow to determine the strength and direction of the regular field component along the line of sight. Dynamo modes of regular fields can be identified from the pattern of polarization angles and of RMs of the diffuse polarized emission of galaxy disks (see Sect. 6.1).

The rotation angle $\Delta\chi$ is proportional to the square of the wavelength λ^2 and the *Faraday depth (FD)*, defined as the line-of-sight integral over the product of the plasma density and the strength of the field component along the line of sight. The *rotation measure (RM)* is defined as $RM = \Delta\chi/\Delta\lambda^2$. If the rotating region is located in front of the emitting region

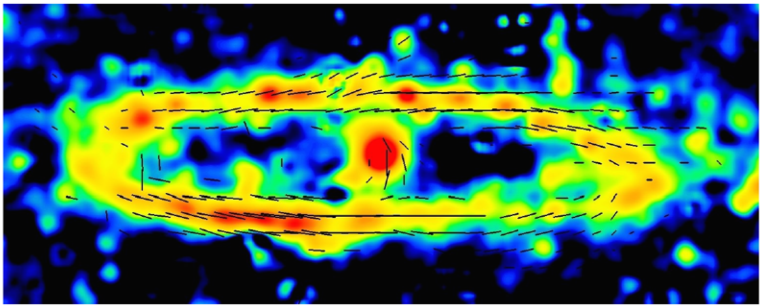

Fig. 1 Total radio intensity (*colors*) and B-vectors (corrected for Faraday rotation) in the Andromeda galaxy (M 31), observed at 6 cm with the Effelsberg telescope (Berkhuijsen et al. 2003)

(*Faraday screen*), $RM = FD$. In case of one region with emission and rotation, $RM \approx FD/2$. Distinct emitting and rotating regions located along the line of sight generate a spectrum of FD components. In such cases, multi-channel spectro-polarimetric radio data are needed that can be Fourier-transformed into Faraday space, called *RM Synthesis* (Brentjens and de Bruyn 2005). If the medium has a relatively simple structure, the 3-D structure of the magnetized interstellar medium can be determined (*Faraday tomography*).

A grid of RM measurements of polarized background sources is another powerful tool to study magnetic field patterns in galaxies (Stepanov et al. 2008). A large number of background sources is required to recognize the field patterns, to separate the Galactic foreground contribution and to account for intrinsic RMs of the background sources.

4 Total Galactic Magnetic Fields

4.1 Total Field Strengths

The typical average *equipartition strength* of the total magnetic field (Beck and Krause 2005) in spiral galaxies is about 10 μG, assuming energy equipartition between cosmic rays and magnetic fields. Radio-faint galaxies like M 31 (Fig. 1) and M 33, our Milky Way's neighbors, have weaker total magnetic fields (about 5 μG), while gas-rich spiral galaxies with high star-formation rates, like M 51 (Fig. 4), M 83 (Fig. 5) and NGC 6946 (Fig. 10), have total field strengths of 20–30 μG in their spiral arms. The strongest total fields of 50–100 μG are found in starburst galaxies, like M 82 (Klein et al. 1988) and the "Antennae" NGC 4038/9 (Chyży and Beck 2004), and in nuclear starburst regions, like in the centers of barred galaxies (Beck et al. 2005).

If energy losses of cosmic-ray electrons are significant, especially in starburst regions or massive spiral arms, the equipartition values are lower limits (Beck and Krause 2005) and are probably underestimated in starburst galaxies by a factor of a few (Thompson et al. 2006). Field strengths of 0.5–18 mG were detected in starburst galaxies by the Zeeman effect in the OH megamaser emission line at 18 cm (Robishaw et al. 2008). These values refer to highly compressed gas clouds and are not typical for the diffuse interstellar medium.

The relative importance of various competing forces in the interstellar medium can be estimated by comparing the corresponding *energy densities*. The mean energy densities of the total (mostly turbulent) magnetic field and the cosmic rays in NGC 6946 (Fig. 2) and M 33 are $\simeq 10^{-11}$ erg cm^{-3} and $\simeq 10^{-12}$ erg cm^{-3}, respectively (Beck 2007; Tabatabaei et

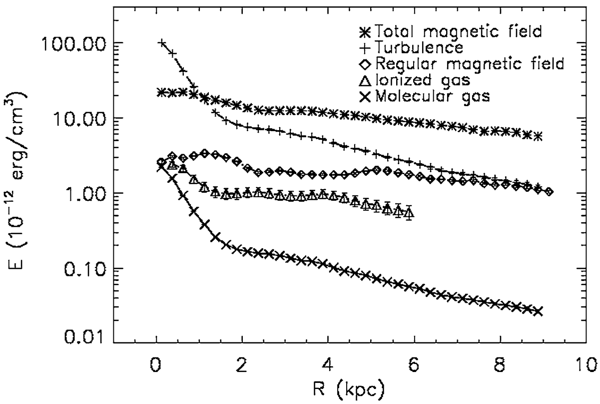

Fig. 2 Radial variation of the energy densities in NGC 6946: total magnetic field E_B ($B_t^2/8\pi$), regular magnetic field ($B_{reg}^2/8\pi$), turbulent motion of the neutral gas E_{turb} ($0.5\rho_n v_{turb}^2$, where $v_{turb} \approx$ 7 km/s), thermal energy of the ionized gas E_{th} ($0.5 n_e k T_e$) and thermal energy of the molecular gas E_n ($0.5 \rho_n k T_n$), determined from observations of synchrotron and thermal radio continuum and the CO and HI line emissions (Beck 2007)

al. 2008), similar to that of the turbulent gas motions across the whole star-forming disk, but about 10 times larger than that of the ionized gas (*low-beta plasma*). Magnetic fields are dynamically important. The total magnetic energy density may even dominate in the outer galaxy where the equipartition field strength is an underestimate due to energy losses of the cosmic-ray electrons. The energy density of the regular magnetic field decreases even more slowly than that of the total field. Although the star-formation activity is low in the outer disk, the magneto-rotational instability (MRI) may serve as the source of turbulence required for dynamo action (Sellwood and Balbus 1999).

4.2 The Radio-Infrared Correlation

The integrated luminosity of the total radio continuum emission at centimeter wavelengths (frequencies of a few GHz), which is mostly of nonthermal synchrotron origin, and the far-infrared (FIR) luminosity of star-forming galaxies are tightly correlated. This correlation is one of the tightest correlations known in astronomy. It extends over five orders of magnitude (Bell 2003) and is valid in starburst galaxies to redshifts of at least 3 (Seymour et al. 2008). Hence the total radio emission can serve as a tracer of magnetic fields and of star formation out to large distances. The correlation requires that total (mostly turbulent) magnetic fields and star formation are connected, so that the field strength exceeds several 100 μG in distant galaxies (Murphy 2009). The tightness needs multiple feedback mechanisms which are not yet understood (Lacki et al. 2010).

The total radio and far-infrared (FIR) or mid-IR (MIR) intensities are also highly correlated within galaxies. The exponent of the correlation in M 51 was found to be different in the central region, spiral arms and interarm regions (Dumas et al. 2011). The radio-infrared correlation can be presented as a correlation between turbulent field strength and star-formation rate (Fig. 3). In contrast, the ordered field is either uncorrelated with the star-formation rate, or anticorrelated in galaxies where the ordered field is strongest in interarm regions with low star formation (Fig. 10). A wavelet cross-correlation analysis for M 33 showed that the radio-FIR correlation holds at all scales down to 1 kpc (Tabatabaei et al. 2007). The correlation in the Large Magellanic Cloud (LMC) breaks down below scales of about 50 pc (Hughes et al. 2006), probably due to the diffusion of cosmic-ray electrons.

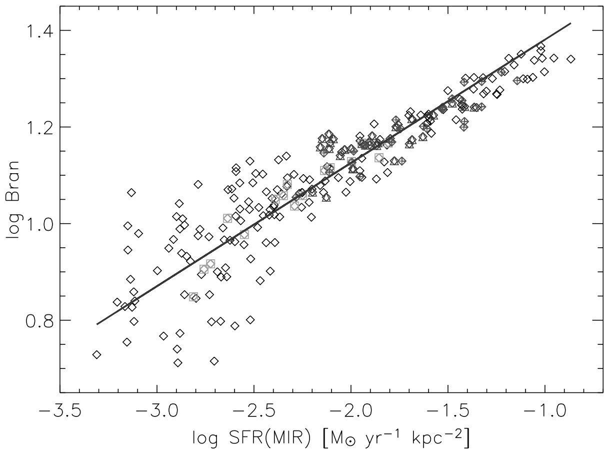

Fig. 3 Correlation between the strength of the total equipartition field (dominated by the turbulent field) and star-formation rate per area (determined from the 24 μm infrared intensities) within the galaxy NGC 4254 (Chyży 2008)

5 Structure of Ordered Galactic Magnetic Fields

5.1 Spiral Galaxies

Ordered (regular and/or anisotropic) field traced by polarized synchrotron emission form spiral patterns in almost every galaxy (Beck 2005), even in ring galaxies (Chyży and Buta 2008), in flocculent galaxies without massive spiral arms (Soida et al. 2002) and in the central regions of galaxies and in circum-nuclear gas rings of barred galaxies (Beck et al. 2005). Ordered fields are generally strongest (10–15 μG) in the regions *between* the optical spiral arms and oriented parallel to the adjacent spiral arms, in some galaxies forming *magnetic arms*, like in IC 342 (Krause 1993) and NGC 6946 (Fig. 10), with exceptionally high degrees of polarization (up to 50%). These are probably generated by a large-scale dynamo (see Sect. 6.1). In galaxies with strong density waves like M 51 (Fig. 4) and M 83 (Fig. 5) enhanced ordered (anisotropic) fields occur at the inner edges of the inner optical arms, in the interarm regions and in the outer optical arms. The observed smooth spiral patterns with significant pitch angles (10°–40°) indicate a general decoupling between magnetic fields and the gas flow, as predicted by mean-field dynamo action. There is no other model to explain the magnetic spiral patterns in many types of galaxies.

The typical degree of radio polarization within the spiral arms is only a few %; hence the field in the spiral arms must be mostly tangled or randomly oriented within the telescope beam, the width of which corresponds to a few 100 pc. Turbulent fields in spiral arms are probably generated by turbulent gas motions related to star formation activity or by a small-scale dynamo.

At wavelengths of around 20 cm, a striking asymmetry of the polarized emission occurs along the major axis of all 12 spiral galaxies observed so far with sufficiently high sensitivity that have inclinations of less than about 60°. The emission is almost completely depolarized by Faraday dispersion always around that side of the major axis which is the kinematically receding one (positive radial velocities) (Braun et al. 2010). In strongly inclined galaxies, both sides of the major axis become Faraday-depolarized at around 20 cm, where most of the polarized emission from the disk is Faraday-depolarized and the emission from the halo field dominates. The asymmetry is still visible at 11 cm wavelength, but disappears at smaller wavelengths. Modeling shows that both, disk and halo field, are of even-symmetry type, as predicted by dynamo models.

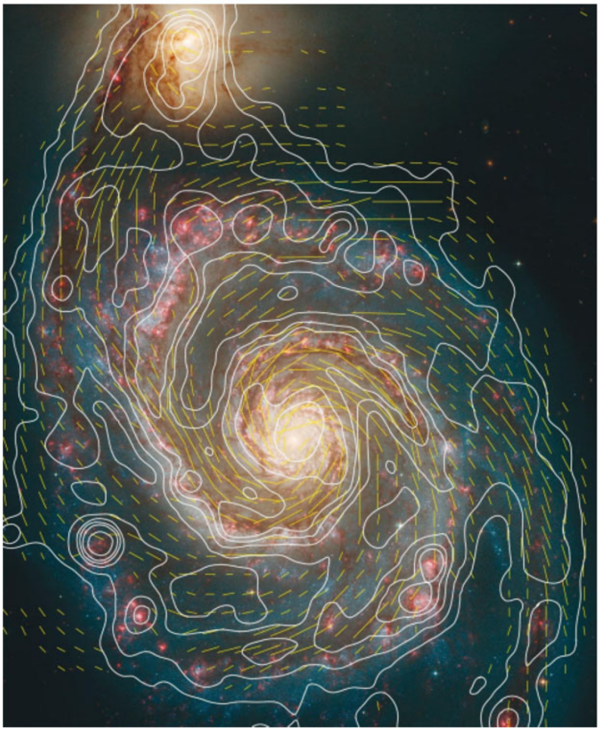

Fig. 4 Total radio emission (*contours*) and *B*-vectors of M 51, combined from observations at 6 cm wavelength with the VLA and Effelsberg telescopes and smoothed to 15” resolution (Fletcher et al. 2011), overlaid onto an optical image from the HST (Copyright: MPIfR Bonn and *Hubble Heritage Team*. Graphics: *Sterne und Weltraum*)

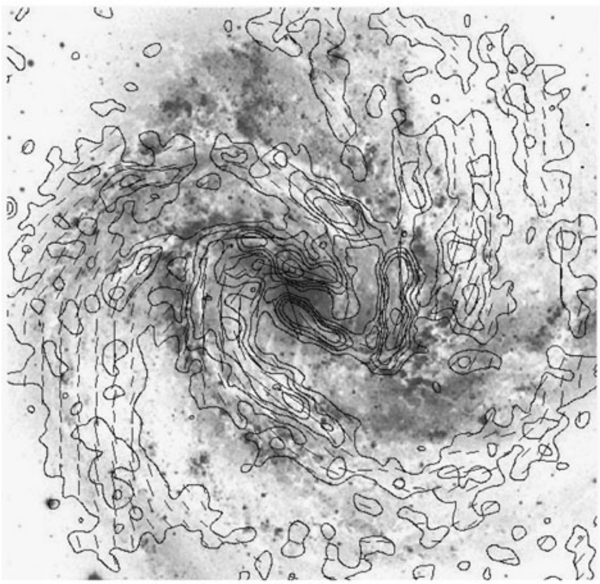

Fig. 5 Polarized radio emission (*contours*) and *B*-vectors of M 83, combined from observations at 6 cm wavelength with the VLA and Effelsberg telescopes and smoothed to 15” resolution (Beck, unpublished), overlaid onto an optical image from Dave Malin (Anglo Australian Observatory)

Fig. 6 Total radio emission (*contours*) and *B*-vectors of the barred galaxy NGC 1097, observed at 6 cm wavelength with the VLA and smoothed to 10" resolution (Beck et al. 2005). The background optical image is from Halton Arp (Copyright: MPIfR Bonn and Cerro Tololo Observatory)

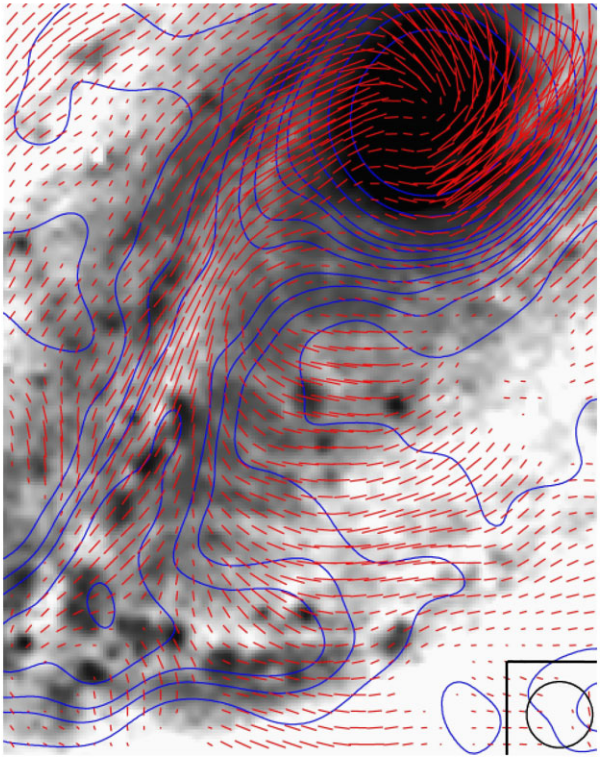

5.2 Barred Galaxies

In galaxies with massive bars the field lines follow the gas flow (Fig. 6). As the gas rotates faster than the bar pattern of a galaxy, a shock occurs in the cold gas that has a small sound speed, while the flow of warm, diffuse gas is only slightly compressed but sheared. The ordered field is also hardly compressed, probably coupled to the diffuse gas and strong enough to affect its flow (Beck et al. 2005). The ordered field is also strong in the upstream region (south of the center in Fig. 6), oriented almost perpendicular to the bar. The polarization pattern in barred galaxies can be used as a tracer of shearing gas flows in the sky plane and complements spectroscopic measurements of radial velocities.

The central regions of barred galaxies are often sites of ongoing intense star formation and strong magnetic fields that can affect the gas flow. NGC 1097 hosts a bright ring with about 1.5 kpc diameter and an active nucleus in its center (Fig. 6). The ordered field in the ring has a spiral pattern and extends towards the nucleus. The orientation of the innermost spiral field agrees with that of the spiral dust filaments visible on optical images. Magnetic stress in the circumnuclear ring due to the strong total magnetic field (about 50 μG) can drive gas inflow (Balbus and Hawley 1998) at a rate of several $M_\odot$/yr, which is sufficient to fuel the activity of the nucleus (Beck et al. 2005).

5.3 Flocculent and Irregular Galaxies

Flocculent galaxies have disks but no prominent spiral arms. Nevertheless, spiral magnetic patterns are observed in all flocculent galaxies, indicative that the mean-field dynamo works

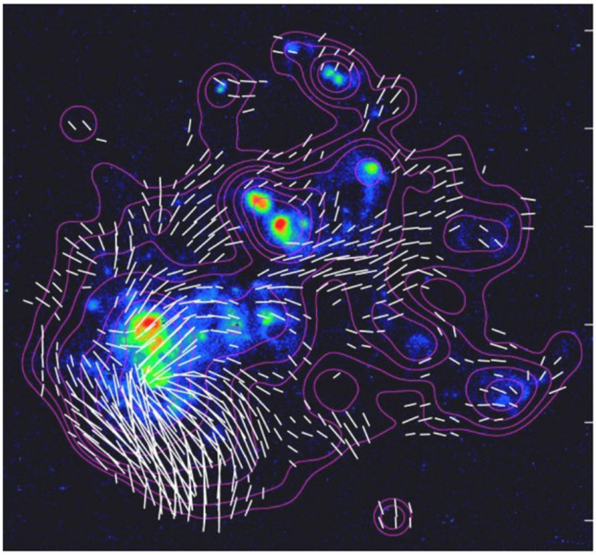

Fig. 7 Total radio intensity (*contours*) and B-vectors of the dwarf irregular galaxy IC 10, observed at 6 cm with the VLA (Chyży 2005). The background Hα image is from Dominik Bomans (Bochum University)

independently of density waves. Ordered magnetic fields with strengths similar to those in grand-design spiral galaxies have been detected in the flocculent galaxies M 33, NGC 3521, NGC 5055 and in NGC 4414 (Soida et al. 2002), and also the mean degree of polarization (corrected for the differences in spatial resolution) is similar between grand-design and flocculent galaxies (Knapik et al. 2000).

Radio continuum maps of irregular, slowly rotating galaxies may reveal strong total equipartition magnetic fields, e.g. in the Magellanic-type galaxy NGC 4449, with a partly ordered field of about 7 μG strength and a spiral pattern (Chyży et al. 2000). Faraday rotation shows that this ordered field is mostly regular and the mean-field dynamo is operating. Dwarf irregular galaxies with almost chaotic rotation do not have any regular fields and only spots of faint polarized emission (Fig. 7). The turbulent field strengths are several times smaller than in spiral galaxies (Chyży et al. 2011), while they are of comparable in starburst dwarfs, e.g. in NGC 1569 with 10–15 μG (Kepley et al. 2010), where star formation activity is sufficiently high for the operation of the small-scale dynamo (Beck et al. 1996).

5.4 Interacting Galaxies

Gravitational interaction between galaxies leads to asymmetric gas flows, compression, shear, enhanced turbulence, and outflows. Compression and shear of gas flows can also modify the structure of galactic and intergalactic magnetic fields. In particular, fields can become aligned along the compression front or perpendicular to the velocity gradients. Such gas flows make turbulent fields highly anisotropic.

The classical interacting galaxy pair is NGC 4038/39, the "Antennae" (Chyży and Beck 2004). It shows bright, extended radio emission filling the whole system. In the interaction region between the galaxies, where star formation did not yet start, and at the northeastern edge of the system, the magnetic field is partly ordered, probably the result of compression and shearing motions along the tidal tail, respectively. Particularly strong, almost unpolarized emission comes from a region of violent star formation, hidden in dust, at the southern end of a dense cloud complex extending between the galaxies. The average total magnetic

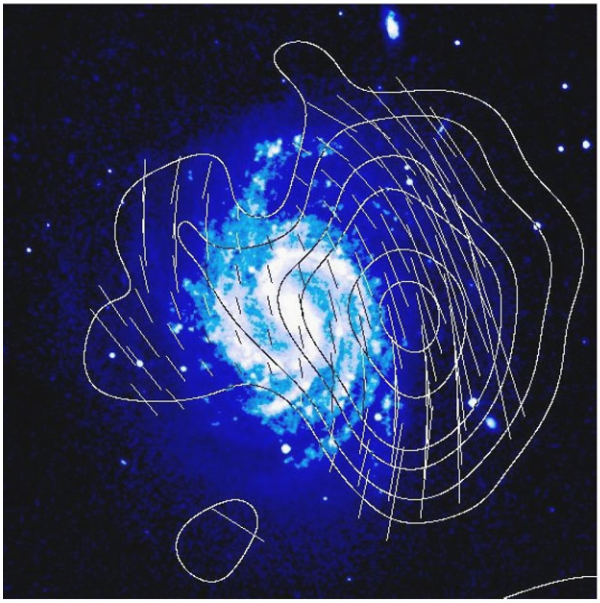

Fig. 8 Polarized radio intensity (*contours*) and *B*-vectors of the Virgo galaxy NGC 4535, observed at 6 cm with the Effelsberg telescope (Weżgowiec et al. 2007). The background optical image is from the Digital Sky Survey

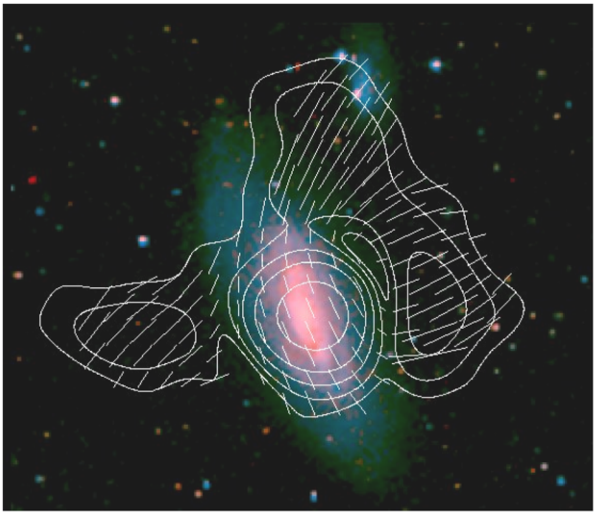

Fig. 9 Polarized radio intensity (*contours*) and *B*-vectors of the Virgo galaxy NGC 4569, observed at 6 cm with the Effelsberg telescope (Chyży et al. 2006). The background optical image is from the Digital Sky Survey

field is stronger than in normal spirals, but the mean degree of polarization is unusually low, implying that the fields are tangled in the regions of violent star formation.

Interaction with a dense intergalactic medium also imprints unique signatures onto magnetic fields and thus the radio emission. The Virgo cluster is a location of especially strong interaction effects (Figs. 8 and 9), and almost all cluster galaxies observed so far show asymmetries of their polarized emission because the outer magnetic fields were compressed (Vollmer et al. 2007). Ordered fields are an excellent tracer of past interactions between galaxies or with the intergalactic medium.

5.5 Edge-on Galaxies

Nearby galaxies seen "edge-on" generally show a disk-parallel field near the disk plane. As a result, polarized emission can be detected from distant, unresolved galaxies if the inclination is larger than about 20° (Stil et al. 2009). This opens a new method to search for ordered fields in distant galaxies. High-sensitivity observations of edge-on galaxies like NGC 891 (Krause 2009) and NGC 253 (Heesen et al. 2009) revealed vertical field components in the halo forming an X-shaped pattern (see Haverkorn and Heesen, this issue).

5.6 Early-Type Galaxies

Spiral galaxies of type Sa and S0 and elliptical galaxies without an active nucleus have very little star formation and hence do not produce cosmic rays that could emit synchrotron emission. The only deep observation of a Sa galaxy, M 104 with a prominent dust ring, revealed weak, ordered magnetic fields (Krause et al. 2006). Large-scale regular magnetic fields may exist in differentially rotating galaxies without star formation because turbulence can be generated by the magneto-rotational instability (MRI) (Sellwood and Balbus 1999). Their detection may become possible via RM grids of background sources with future radio telescopes (see Sect. 7).

6 Faraday Rotation

6.1 Large-Scale Regular Fields

Spiral fields are generated by compression, by shear in interarm regions, or by dynamo action (Sect. 2). Large-scale patterns of Faraday rotation measures (RM) are signatures of the mean-field dynamo and can be identified from diffuse polarized emission of the galaxy disks (Krause 1990) or from RM data of polarized background sources (Stepanov et al. 2008). If several dynamo modes are superimposed, a Fourier analysis of the RM variation is needed. The resolution of present-day observations is sufficient to identify 2–3 modes.

The disks of about a dozen nearby spiral galaxies reveal large-scale RM patterns. The Andromeda galaxy M 31 (Fig. 1) is the prototype of a dynamo-generated axisymmetric spiral disk field (Fletcher et al. 2004). Other candidates for a dominating axisymmetric disk field (dynamo mode $m = 0$) are the nearby spiral IC 342 (Krause et al. 1989a) and the irregular Large Magellanic Cloud (LMC) (Gaensler et al. 2005). Dominating bisymmetric spiral fields (dynamo mode $m = 1$) are rare, as predicted by dynamo models. Faraday rotation in NGC 6946 (Fig. 11) and in other similar galaxies with magnetic arms can be described by a superposition of two azimuthal dynamo modes ($m = 0$ and $m = 2$) with about equal amplitudes where the quadrisymmetric spiral mode is phase shifted with respect to the density wave (Beck 2007).

However, the spiral pattern of magnetic fields cannot be solely the result of mean-field dynamo action. If the beautiful spiral pattern of M 51 seen in radio polarization (Fig. 4) were only due to a regular field, its line-of sight component should generate a conspicuous large-scale pattern in Faraday rotation, which is not observed. This means that a large amount of the ordered field is anisotropic and probably generated by compression and shear of the non-axisymmetric gas flows in the density-wave potential. The anisotropic field is strongest at the positions of the prominent dust lanes on the inner edge of the inner gas spiral arms, due to compression of turbulent fields in the density-wave shock. Regular fields (dynamo modes

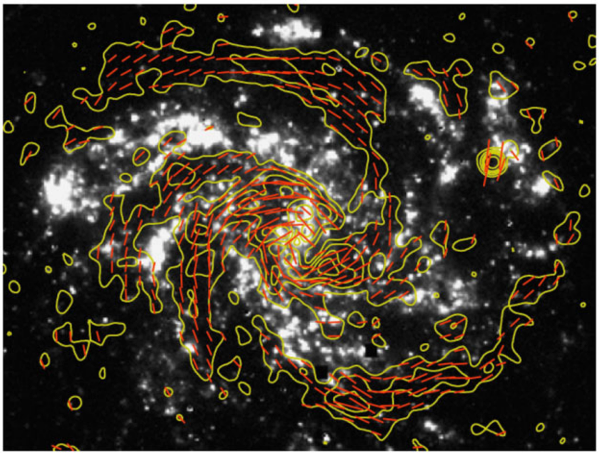

Fig. 10 Polarized radio emission (*contours*) and B-vectors of NCC 6946, combined from observations at 6 cm wavelength with the VLA and Effelsberg telescopes and smoothed to 15” resolution (Beck 2007), overlaid onto an Hα image from Anne Ferguson (Copyright: MPIfR Bonn; graphics: *Sterne und Weltraum*)

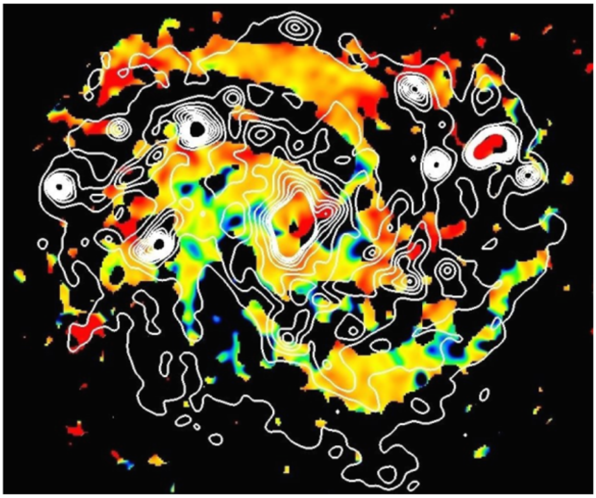

Fig. 11 Total radio intensity at 6 cm wavelength (*contours*) and Faraday rotation measures between 3.6 cm and 6 cm wavelengths (*colors*) in NGC 6946, derived from combined observations with the VLA and Effelsberg telescopes (Beck 2007). The colour scale ranges from -75 rad/m^2 to $+175$ rad/m^2. The average rotation measure of about $+50$ rad/m^2 is caused by the foreground medium in the Milky Way

$m = 0$ and $m = 1$) also exist in the disk of M 51, but are much weaker than the anisotropic field (Fletcher et al. 2011).

In many other observed galaxy disks no clear patterns of Faraday rotation were found. Either several dynamo modes are superimposed and cannot be distinguished with the limited sensitivity and resolution of present-day telescopes, or the timescale for the generation of large-scale modes is longer than the galaxy's lifetime (Arshakian et al. 2009).

By measuring the signs of the RM distribution and the velocity field on both sides of a galaxy's major axis, the inward and outward directions of the radial component of the axisymmetric field can be easily distinguished (Krause and Beck 1998). Dynamo models predict that both signs have the same probability, which is confirmed by observations. The axisymmetric fields of M 31, IC 342, NGC 253 and the axisymmetric field component in NGC 6946 point inwards, while those of NGC 4254, NGC 5775 and the axisymmetric component of the disk field in M 51 point outwards.

While the azimuthal symmetry of the magnetic field is known for many galaxies, the vertical symmetry (even or odd) is much harder to determine. The RM patterns of even and odd modes are similar in mildly inclined galaxies. The field of odd modes reverses its sign above and below the galactic plane. The symmetry type becomes only visible in strongly inclined galaxies, as the RM sign above and below the plane (see Haverkorn and Heesen, this issue).

6.2 Field Reversals

Large-scale field reversals at certain radial distances from a galaxy's center, like those in the Milky Way (Noutsos, this issue), have not been detected in spiral galaxies, although high-resolution RM maps of Faraday rotation are available for many spiral galaxies. In M 81 the dominating BSS field implies two large-scale reversals (Krause et al. 1989b). A satisfying explanation for the reversals in the Milky Way is still lacking. They may be restricted to a thin layer near to the plane and hence are hardly visible in the average RM data of external galaxies along the line of sight. Secondly, the reversals in the Milky Way may be of limited azimuthal extent and are difficult to observe in external galaxies with present-day telescopes. In the barred galaxy NGC 7479, where a jet serves as a bright polarized background and high-resolution observations were possible with high signal-to-noise ratio, several reversals on 1–2 kpc scale were detected in the foreground disk of the galaxy (Laine and Beck 2008). Thirdly, the reversals in the Milky Way may be part of a disturbed field structure, e.g. due to interaction with the Magellanic clouds.

7 Outlook

Future high-resolution, high-sensitivity observations at high frequencies with the *Extended Very Large Array* (EVLA) and the planned *Square Kilometre Array* (SKA) will directly map the detailed field structure and the interaction with the gas. The low-frequency radio telescopes *Low Frequency Array* (LOFAR) and the *Murchison Widefield Array* (MWA) (under construction) are suitable instruments to search for extended synchrotron radiation at the lowest possible levels in outer galaxy disks and halos and the transition to intergalactic space. Low frequencies are also ideal to search for small Faraday rotation measures from weak interstellar and intergalactic fields (Beck 2009).

Total synchrotron emission, signature of total magnetic fields, can be detected with the SKA out to very large redshifts for starburst galaxies, depending on luminosity and magnetic field strength (Fig. 12). However, for fields weaker than 3.25 μG $(1+z)^2$, energy loss of cosmic-ray electrons is dominated by the inverse Compton effect with CMB photons, so that their energy appears mostly in X-rays and not in the radio range. On the other hand, for strong magnetic fields the energy range of the electrons emitting at 1.4 GHz shifts to low energies where ionization and bremsstrahlung losses become dominant. In summary, the mere detection of synchrotron emission at high redshifts will constrain the allowed magnetic field strengths in young galaxies.

If polarized emission from galaxies is too weak to be detected, the method of *RM grids* towards background QSOs can still be applied. Here, the distance limit is given by the polarized flux of the background QSO which can be much higher than that of the intervening galaxy. Significant regular fields of several μG strength were already detected in distant galaxies (Bernet et al. 2008). Mean-field dynamo theory predicts RMs from evolving regular fields with increasing coherence scale at $z \leq 3$ (Arshakian et al. 2009). The RM values are reduced by the redshift dilution factor of $(1+z)^{-2}$.

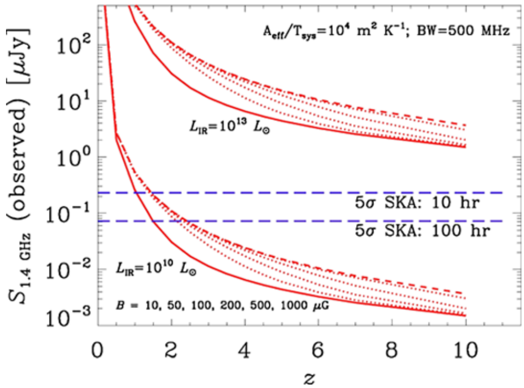

Fig. 12 Total synchrotron emission at 1.4 GHz as a function of redshift z and magnetic field strength B, and the 5σ detection limits for 10 h and 100 h integration time with the SKA (Murphy 2009)

Fig. 13 Simulation of RMs towards background sources (*white points*) in the region of M 31 observable with the SKA within 1 h. Optical emission from M 31 is shown in *red*, diffuse radio continuum intensity in *blue* and diffuse polarized intensity in *green* (from Gaensler, priv. comm.)

Faraday rotation in the direction of QSOs allows to determine the strength and pattern of a regular field in an intervening galaxy (Kronberg et al. 1992). A reliable model for the field structure of galaxies needs RM values from a large number of polarized background sources, hence large sensitivity and/or high survey speed.

The planned all-sky POSSUM survey at 1.4 GHz with the *Australia SKA Pathfinder* (ASKAP) telescope (under construction) with 30 deg^2 field of view (Gaensler et al. 2010) will measure about 100 RM values from polarized extragalactic sources per square degree within 10 h integration time. Similarly long integrations with the EVLA and with MeerKAT will show more sources, but their fields of view are smaller.

The SKA "Magnetism" Key Science Project plans to observe an all-sky survey (at least 10^4 deg^2) around 1 GHz with 1 h integration per field which will be able to detect sources of 0.5–1 μJy flux density and measure at least 1500 RMs per square degree. This will contain at least 2×10^7 RMs from compact polarized extragalactic sources at a mean spacing of $\simeq 90''$ (Gaensler et al. 2004). More than 10 000 RM values are expected in the area of M 31 (Fig. 13) and will allow the detailed reconstruction of the 3-D field structure in this and many other nearby galaxies, while simple patterns of regular fields can be recognized out to distances of about 100 Mpc (Stepanov et al. 2008).

We are entering a golden era of magnetic field observations in galaxies.

Acknowledgements ISSI Bern and Prof. Dr. André Balogh is acknowledged for hospitality and financial support. The author thanks Dr. Marita Krause for careful reading of the manuscript.

References

P. Abreu et al. (The Pierre Auger Collaboration), Astropart. Phys. **34**, 314 (2010)
T.G. Arshakian, R. Beck, M. Krause, D. Sokoloff, Astron. Astrophys. **494**, 21 (2009)
S.A. Balbus, J.F. Hawley, Rev. Mod. Phys. **70**, 1 (1998)
R. Beck, in *Cosmic Magnetic Fields*, ed. by R. Wielebinski, R. Beck (Springer, Berlin, 2005), p. 41
R. Beck, Astron. Astrophys. **470**, 539 (2007)
R. Beck, Rev. Mex. Astron. Astrof. **36**, 1 (2009)
R. Beck, M. Krause, Astron. Nachr. **326**, 414 (2005)
R. Beck, A. Brandenburg, D. Moss, A. Shukurov, D. Sokoloff, Annu. Rev. Astron. Astrophys. **34**, 155 (1996)
R. Beck, A. Fletcher, A. Shukurov et al., Astron. Astrophys. **444**, 739 (2005)
E.F. Bell, Astrophys. J. **586**, 794 (2003)
E.M. Berkhuijsen, R. Beck, P. Hoernes, Astron. Astrophys. **398**, 937 (2003)
M.L. Bernet, F. Miniati, S.J. Lilly, P.P. Kronberg, M. Dessauges-Zavadsky, Nature **454**, 302 (2008)
A. Brandenburg et al., Space Sci. Rev. (2011, this issue)
R. Braun, G. Heald, R. Beck, Astron. Astrophys. **514**, A42 (2010)
M.A. Brentjens, A.G. de Bruyn, Astron. Astrophys. **441**, 1217 (2005)
C. Caprini, R. Durrer, E. Fenu, J. Cosmol. Astropart. Phys. **11**, 001 (2009)
K.T. Chyży, in *From 30 Doradus to Lyman Break Galaxies*, ed. by R. de Grijs, R.M. González Delgado (Springer, Berlin, 2005), p. 12
K.T. Chyży, Astron. Astrophys. **482**, 755 (2008)
K.T. Chyży, R. Beck, Astron. Astrophys. **417**, 541 (2004)
K.T. Chyży, R.J. Buta, Astrophys. J. **677**, L17 (2008)
K.T. Chyży, R. Beck, S. Kohle, U. Klein, M. Urbanik, Astron. Astrophys. **356**, 757 (2000)
K.T. Chyży, M. Soida, D.J. Bomans et al., Astron. Astrophys. **447**, 465 (2006)
K.T. Chyży, M. Weżgowiec, R. Beck, D.J. Bomans, Astron. Astrophys. **529**, A94 (2011)
K. Dolag, M. Kachelriess, S. Ostapchenko, R. Tomas, Astrophys. J. **727**, L4 (2011)
G. Dumas, E. Schinnerer, F.S. Tabatabaei et al., Astron. J. **141**, 41 (2011)
A. Fletcher, E.M. Berkhuijsen, R. Beck, A. Shukurov, Astron. Astrophys. **414**, 53 (2004)
A. Fletcher, R. Beck, A. Shukurov, E.M. Berkhuijsen, C. Horellou, Mon. Not. R. Astron. Soc. **412**, 2396 (2011)
P. Fosalba, A. Lazarian, S. Prunet, J.A. Tauber, Astrophys. J. **546**, 762 (2002)
B.M. Gaensler, R. Beck, L. Feretti, in *Science with the Square Kilometer Array*, ed. by C. Carilli, S. Rawlings. New Astr. Rev., vol. 48 (Elsevier, Amsterdam, 2004), p. 1003
B.M. Gaensler, M. Haverkorn, L. Staveley-Smith et al., Science **307**, 1610 (2005)
B.M. Gaensler, T.L. Landecker, A.R. Taylor, Bull. Am. Astron. Soc. **42**, 470 (2010)
C. Gissinger, S. Fromang, E. Dormy, Mon. Not. R. Astron. Soc. **394**, L84 (2009)
J.S. Greaves, W.S. Holland, T. Jenness, T.G. Hawarden, Nature **404**, 732 (2000)
O. Gressel, D. Elstner, U. Ziegler, G. Rüdiger, Astron. Astrophys. **486**, L35 (2008)
M. Hanasz, D. Wóltański, K. Kowalik, Astrophys. J. **706**, L155 (2009)
H. Hanayama, K. Takahashi, K. Kotake et al., Astrophys. J. **633**, 941 (2005)
M. Haverkorn, V. Heesen, Space Sci. Rev. (2011, this issue). doi:10.1007/s11214-011-9757-0
V. Heesen, M. Krause, R. Beck, R.-J. Dettmar, Astron. Astrophys. **506**, 1123 (2009)
C. Heiles, Space Sci. Rev. (2011, this issue)
A. Hughes, T. Wong, R. Ekers et al., Mon. Not. R. Astron. Soc. **370**, 363 (2006)
A.A. Kepley, S. Mühle, J. Everett et al., Astrophys. J. **712**, 536 (2010)
U. Klein, R. Wielebinski, H. Morsi, Astron. Astrophys. **190**, 41 (1988)
J. Knapik, M. Soida, R.-J. Dettmar, R. Beck, M. Urbanik, Astron. Astrophys. **362**, 910 (2000)
F. Krause, R. Beck, Astron. Astrophys. **335**, 789 (1998)
M. Krause, in *Galactic and Intergalactic Magnetic Fields*, ed. by R. Beck et al. (Kluwer, Dordrecht, 1990), p. 187

M. Krause, in *The Cosmic Dynamo*, ed. by F. Krause et al. (Kluwer, Dordrecht, 1993), p. 303
M. Krause, Rev. Mex. Astron. Astrof. **36**, 25 (2009)
M. Krause, E. Hummel, R. Beck, Astron. Astrophys. **217**, 4 (1989a)
M. Krause, R. Beck, E. Hummel, Astron. Astrophys. **217**, 17 (1989b)
M. Krause, R. Wielebinski, M. Dumke, Astron. Astrophys. **448**, 133 (2006)
P.P. Kronberg, J.J. Perry, E.L.H. Zukowski, Astrophys. J. **387**, 528 (1992)
B.C. Lacki, T.A. Thompson, E. Quataert, Astrophys. J. **717**, 1 (2010)
S. Laine, R. Beck, Astrophys. J. **673**, 128 (2008)
M. Lazar, R. Schlickeiser, R. Wielebinski, S. Poedts, Astrophys. J. **693**, 1133 (2009)
E. Murphy, Astrophys. J. **706**, 482 (2009)
A. Noutsos, Space Sci. Rev. (2011, this issue)
M.J. Rees, in *Cosmic Magnetic Fields*, ed. by R. Wielebinski, R. Beck (Springer, Berlin, 2005), p. 1
T. Robishaw, E. Quataert, C. Heiles, Astrophys. J. **680**, 981 (2008)
S.M. Scarrott, D. Ward-Thompson, R.F. Warren-Smith, Mon. Not. R. Astron. Soc. **224**, 299 (1987)
D.R.G. Schleicher, R. Banerjee, S. Sur et al., Astron. Astrophys. **522**, A115 (2010)
J.A. Sellwood, S.A. Balbus, Astrophys. J. **511**, 660 (1999)
N. Seymour, T. Dwelly, D. Moss et al., Mon. Not. R. Astron. Soc. **386**, 1695 (2008)
A. Shukurov, D. Sokoloff, K. Subramanian, A. Brandenburg, Astron. Astrophys. **448**, L33 (2006)
M. Soida, R. Beck, M. Urbanik, J. Braine, Astron. Astrophys. **394**, 47 (2002)
D.D. Sokoloff, A.A. Bykov, A. Shukurov et al., Mon. Not. R. Astron. Soc. **299**, 189 (1998). Erratum in Mon. Not. R. Astron. Soc. **303**, 207 (1999)
R. Stepanov, T.G. Arshakian, R. Beck, P. Frick, M. Krause, Astron. Astrophys. **480**, 45 (2008)
J.M. Stil, M. Krause, R. Beck, A.R. Taylor, Astrophys. J. **693**, 1392 (2009)
F. Tabatabaei, R. Beck, M. Krause et al., Astron. Astrophys. **466**, 509 (2007)
F. Tabatabaei, M. Krause, A. Fletcher, R. Beck, Astron. Astrophys. **490**, 1005 (2008)
J.-W. Tang, P.T.P. Ho, P.M. Koch et al., Astrophys. J. **700**, 251 (2009)
T.A. Thompson, E. Quataert, E. Waxman, N. Murray, C.L. Martin, Astrophys. J. **645**, 186 (2006)
B. Vollmer, M. Soida, R. Beck et al., Astron. Astrophys. **464**, L37 (2007)
M. Weżgowiec, M. Urbanik, B. Vollmer et al., Astron. Astrophys. **471**, 93 (2007)
L.M. Widrow, Rev. Mod. Phys. **74**, 775 (2002)